2006

The effect of calcium on aqueous uranium(VI) speciation and adsorption to ferrihydrite and quartz

Patricia M. Fox
U.S. Geological Survey, pfox@usgs.gov

James A. Davis
U.S. Geological Survey

John M. Zachara
Pacific Northwest National Laboratory, john.zachara@pnl.gov

Available online at www.sciencedirect.com
SCIENCE DIRECT
Geochimica et Cosmochimica Acta 70 (2006) 1379–1387
Geochimica
www.elsevier.com/locate/gca

The effect of calcium on aqueous uranium(VI) speciation and adsorption to ferrihydrite and quartz

Patricia M. Fox [a,*], James A. Davis [a], John M. Zachara [b]

[a] U.S. Geological Survey, 345 Middlefield Road. MS 465, Menlo Park, CA 94025, USA
[b] Pacific Northwest National Laboratory, P.O. Box 999, Richland, WA 99338, USA

Received 22 July 2005; accepted in revised form 22 November 2005

Abstract

Recent studies of uranium(VI) geochemistry have focused on the potentially important role of the aqueous species, $CaUO_2(CO_3)_3^{2-}$ and $Ca_2UO_2(CO_3)_3^0(aq)$, on inhibition of microbial reduction and uranium(VI) aqueous speciation in contaminated groundwater. However, to our knowledge, there have been no direct studies of the effects of these species on U(VI) adsorption by mineral phases. The sorption of U(VI) on quartz and ferrihydrite was investigated in $NaNO_3$ solutions equilibrated with either ambient air (430 ppm CO_2) or 2% CO_2 in the presence of 0, 1.8, or 8.9 mM Ca^{2+}. Under conditions where the $Ca_2UO_2(CO_3)_3^0(aq)$ species predominates U(VI) aqueous speciation, the presence of Ca in solution lowered U(VI) adsorption on quartz from 77% in the absence of Ca to 42% and 10% at Ca concentrations of 1.8 and 8.9 mM, respectively. U(VI) adsorption to ferrihydrite decreased from 83% in the absence of Ca to 57% in the presence of 1.8 mM Ca. Surface complexation model predictions that included the formation constant for aqueous $Ca_2UO_2(CO_3)_3^0(aq)$ accurately simulated the effect of Ca^{2+} on U(VI) sorption onto quartz and ferrihydrite within the thermodynamic uncertainty of the stability constant value. This study confirms that Ca^{2+} can have a significant impact on the aqueous speciation of U(VI), and consequently, on the sorption and mobility of U(VI) in aquifers.

1. Introduction

Uranium contamination of soils and groundwaters occurs at mining and mill sites throughout the USA. It is an important contaminant at many US Department of Energy sites resulting from the storage, disposal, and processing of nuclear materials (Riley et al., 1992; Crowley and Ahearne, 2002). Under oxidizing conditions uranium, present as U(VI), can be quite mobile in aquifers (Davis and Curtis, 2003; Curtis et al., 2004; Kohler et al., 2004). The mobility of uranium (U) in water-rock systems is controlled both by precipitation reactions and by sorption reactions with mineral surfaces. A fundamental understanding of the sorption behavior of U in water-mineral systems is necessary for accurate risk assessments to be performed at uranium-contaminated sites.

It has been concluded in many U(VI) sorption studies that the mobility of U(VI) in aquifers with circumneutral to alkaline pH values is due to the formation of the uranyl-carbonato complexes, $UO_2(CO_3)_2^{2-}$ and $UO_2(CO_3)_3^{4-}$ (Hsi and Langmuir, 1985; Waite et al., 1994; Pabalan et al., 1998; Barnett et al., 2000). However, recent evidence indicates that calcium uranyl carbonate complexes [$Ca_2UO_2(CO_3)_3^0(aq)$; $CaUO_2(CO_3)_3^{2-}$] may play an important role in the aqueous chemistry of U(VI) at alkaline pH values because of their large formation constants (Bernhard et al., 1996, 2001; Kalmykov and Choppin, 2000). These complexes have recently been identified by extended X-ray absorption fine structure (EXAFS) spectroscopy in calcium-rich waters (2–5 mM Ca), directly observed in contaminated vadose zone porewaters at the US DOE Hanford site by laser-induced fluorescence spectroscopy, and have been shown to inhibit microbial reduction of U(VI) under certain conditions (Bernhard et al., 2001; Brooks et al., 2003; Wang et al., 2004). In addition,

* Corresponding author. Fax: +1 650 329 4545.
E-mail address: pfox@usgs.gov (P.M. Fox).

0016-7037/$ - see front matter © 2006 Elsevier Inc. All rights reserved.
doi:10.1016/j.gca.2005.11.027

thermodynamic calculations suggest that the calcium uranyl carbonate complexes may be the predominant forms of dissolved U(VI) in many U(VI)-contaminated groundwaters (Brooks et al., 2003; Davis and Curtis, 2003; Davis et al., 2004).

Numerous investigations of U(VI) sorption are described in the literature, including experiments on natural soils and sediments (Duff and Amrhein, 1996; Turner et al., 1996; Barnett et al., 2000, 2002; Zheng et al., 2003; Davis et al., 2004) and on pure mineral phases such as amorphous iron oxides, carbonates, and hematite (Hsi and Langmuir, 1985; Waite et al., 1994; Duff and Amrhein, 1996; Pabalan et al., 1998; Payne, 1999). Investigators have examined the effects of ionic strength, partial pressure of carbon dioxide, and pH. Most of these studies of U(VI) sorption on pure mineral phases were performed in simple electrolyte solutions (e.g., $NaNO_3$ and NaCl) (Hsi and Langmuir, 1985; Waite et al., 1994; Kohler et al., 1996). However, natural systems are much more complex, containing a variety of organic and inorganic ions in solution. Bivalent cations, such as Ca, may affect the adsorption of U(VI) in several ways, including competing with uranyl cations for sorption sites, changing the surface charge or potential of minerals, and affecting the aqueous speciation of U(VI), via the formation of the calcium uranyl carbonate complexes.

There is very little information in the literature on the effect of Ca on U(VI) sorption. Zheng et al. (2003) found that the presence of calcium carbonate in soils decreased U(VI) sorption and attributed this effect to the presence of calcium uranyl carbonate complexes. Hsi and Langmuir (1985) saw no effect of 1 mM Ca or Mg on U(VI) sorption by iron oxides in carbonate-free systems, while Duff and Amrhein (1996) observed lower U(VI) sorption to goethite in synthetic drainage waters containing elevated levels of Ca (11–19 mM) and Mg (4–6 mM). They attributed this effect to competition between Ca and Mg ions and positively charged U(VI) species for surface sites. In light of the recent identification of $Ca_2UO_2(CO_3)_3^0$(aq) as an important U(VI) species, however, observations of decreased U(VI) adsorption could also be attributed to the presence of non-adsorbing, aqueous calcium uranyl carbonate complexes. Thus, a better understanding of the effect of Ca on U(VI) sorption, particularly in pure mineral systems where a number of variables can be easily constrained, is needed to create more accurate models of U(VI) mobility in contaminated groundwater. In this study, we determined the effect of calcium on the adsorption of U(VI) by ferrihydrite and quartz, two important mineral phases in natural systems.

2. Materials and methods

2.1. Solids

Two-line ferrihydrite was synthesized by titrating a solution of $Fe(NO_3)_3$ with 1 M NaOH to pH 6 while stirring rapidly (Waite et al., 1994). The slurry was aged for 65 h at 25 °C in a water bath. The ferrihydrite slurry, which had a final iron concentration of 0.1 M and a nitrate concentration of 0.3 M was diluted to 10^{-3} or 10^{-4} M Fe for U(VI) sorption experiments.

The quartz used in this experiment was Min-U-Sil 30 (Pennsylvania Glass & Sand Company), a crushed quartz powder. Quartz was treated to remove contaminants as described by Kohler et al. (1996). Grain sizes were 8–30 μm and the specific surface area as measured by BET krypton gas adsorption was 0.32 m^2/g.

2.2. Batch experiments

Five sets of aqueous chemical conditions were used in the quartz and ferrihydrite sorption experiments: (1) 5, 10.9, or 32 mM $NaNO_3$ solution with no added Ca^{2+}; equilibrated with air (to study ionic strength dependence), (2) 5 mM $NaNO_3$ solution with 1.8 mM added $Ca(NO_3)_2$; equilibrated with air, (3) 5 mM $NaNO_3$ solution with 8.9 mM added $Ca(NO_3)_2$; equilibrated with air, (4) 5 mM $NaNO_3$ solution equilibrated with a 2%/98% CO_2/N_2 gas mixture, and (5) 5 mM $NaNO_3$ solution with 1.8 mM added $Ca(NO_3)_2$; equilibrated with a 2%/98% CO_2/N_2 gas mixture. The pH range studied was limited on the alkaline side by calcite precipitation, which is predicted to occur at pH 7.99, 7.69, and 7.18, for solutions 2, 3, and 5, respectively. Experiments were conducted at elevated ionic strength using 32 and 10.9 mM $NaNO_3$ (in the absence of Ca^{2+}) for quartz and ferrihydrite, respectively, to verify that the increased ionic strength in the Ca^{2+}-bearing solutions had no effect on U(VI) sorption in this pH range. For quartz, experiments were also conducted with the addition of dissolved silicate to check for any influence of silicate on U(VI) sorption. The ferrihydrite experiments were performed in 250 mL HDPE centrifuge bottles that were equipped with inlet and outlet tubes to allow for bubbling of the air mixture, either ambient laboratory air [430 ppm CO_2 (v/v)] or 2% CO_2. The 2% CO_2 mixture was a commercially prepared gas mixture consisting of 2% CO_2 with the balance air (actual CO_2 concentration was 2.007–2.047%, depending on the tank). All gas mixtures were filtered (0.45 μm nylon) and humidified before bubbling into the samples to prevent contamination and evaporative loss. The bubbling also served to mix the samples throughout the experiment. The experiments were performed at 25 °C in a water bath. Quartz experiments were performed in 35 mL polycarbonate centrifuge tubes in laboratory air only. Samples were mixed by an end-over-end rotator. No temperature control was used for the quartz experiments, and the temperature in the laboratory was 21 ± 2 °C.

Aliquots of the stirred ferrihydrite slurry were transferred to the reaction vessels using an autopipet to achieve a final concentration of 10^{-3} or 10^{-4} M Fe. Quartz was weighed directly into the centrifuge tubes to achieve 25 g/L. Enough $NaNO_3$ was added to each reaction vessel to reach

the desired concentration, taking into account the $NaNO_3$ already present in the diluted ferrihydrite slurry. An appropriate amount of $NaHCO_3$ was added to achieve equilibrium with the partial pressure of CO_2 at the desired pH. Experiments with calcium were spiked with a 0.1 M $Ca(NO_3)_2$ stock solution to achieve a final Ca concentration of 1.8 or 8.9 mM. For experiments with dissolved silicate, samples were spiked with a 1 mM Na_2SiO_3 solution to achieve final dissolved Si concentrations of 0.030–0.147 mM. The exact Si concentrations were designed to simulate the dissolved Si measured in batch experiments with 8.9 mM Ca, which increased with increasing pH. The samples were immediately bubbled with the appropriate gas mixture for 1 h before the pH was adjusted using 0.1 M HNO_3 and NaOH, if necessary. When pH adjustment was necessary, only microliter quantities of acid or base were added, corresponding to a change in ionic strength of no more than 3.0×10^{-5} M. For all pH measurements and adjustments in the elevated CO_2 experiments, the exposure to air was minimized (no more than 5 min) to prevent the solution from equilibrating with air rather than 2% carbon dioxide. The samples were then allowed to equilibrate for 24 h before U(VI) was added. Ferrihydrite samples were continuously bubbled with the gas mixture throughout the experiment in a 25 °C water bath, while quartz samples were capped and mixed after an additional 2 h of bubbling.

After the 24 h equilibration, each sample was spiked with a $UO_2(NO_3)_2$ stock solution to achieve a U(VI) concentration of 10^{-6} M. When necessary, the pH was then readjusted with 0.1 M NaOH or HNO_3 to the value measured just before spiking with U(VI). After 48 h, pH was measured and samples were centrifuged at 26,890*g* for 10 min to separate the solid and liquid phases. The 48-h reaction time was based on the kinetic data of Waite et al. (1994) and M. Kohler (quartz, unpublished results) in the absence of calcium, as well as kinetic data presented here for U(VI) sorption in the presence of calcium. For selected samples, a 5-mL solution aliquot was removed for alkalinity measurements (by Gran titration). After removing the aliquot for alkalinity, the remaining solution sample was acidified to 0.15 M HNO_3 for uranium and major ion (Ca, Na, Fe, and Si) analysis by the kinetic phosphorescence analyzer (KPA) and inductively coupled plasma atomic emission spectrometry (ICP-AES), respectively. Alkalinity measurements were checked against expected alkalinity calculated for each sample by FITEQL 4.0 (Herbelin and Westall, 1999), based on the measured pH and known pCO_2 value, to verify that the system was near equilibrium with respect to the partial pressure of CO_2 in the gas phase. The results are shown in Tables 1 and 2 along with pH and ionic strength.

2.3. Modeling

FITEQL 4.0 (Herbelin and Westall, 1999) was used for aqueous speciation and surface complexation modeling.

Table 1
pH, ionic strength, and alkalinity for quartz samples equilibrated with air (430 ppm CO_2)

pH	Ionic strength (M)	Measured alkalinity (eq/L)	Calculated alkalinity (eq/L)
5 mM $NaNO_3$, zero Ca			
7.08	5.08×10^{-3}	7.84×10^{-5}	8.32×10^{-5}
7.38	5.17×10^{-3}	1.62×10^{-4}	1.67×10^{-4}
7.68	5.33×10^{-3}	3.30×10^{-4}	3.35×10^{-4}
7.86	5.53×10^{-3}	4.81×10^{-4}	5.13×10^{-4}
7.94	5.61×10^{-3}	6.01×10^{-4}	6.13×10^{-4}
8.50	7.46×10^{-3}	2.16×10^{-3}	2.34×10^{-3}
8.69	8.85×10^{-3}	3.61×10^{-3}	3.65×10^{-3}
5 mM $NaNO_3$, 1.8 mM $Ca(NO_3)_2$			
7.01	1.04×10^{-2}	7.05×10^{-5}	7.39×10^{-5}
7.35	1.05×10^{-2}	1.67×10^{-4}	1.62×10^{-4}
7.50	1.06×10^{-2}	2.20×10^{-4}	2.27×10^{-4}
7.72	1.07×10^{-2}	3.77×10^{-4}	3.81×10^{-4}
7.95	1.10×10^{-2}	6.60×10^{-4}	6.52×10^{-4}
5 mM $NaNO_3$, 8.9 mM $Ca(NO_3)_2$			
6.97	3.18×10^{-2}	7.90×10^{-5}	7.17×10^{-5}
7.21	3.18×10^{-2}	1.25×10^{-4}	1.25×10^{-4}
7.41	3.19×10^{-2}	2.22×10^{-4}	1.98×10^{-4}
7.68	3.21×10^{-2}	3.48×10^{-4}	3.67×10^{-4}
7.95	3.23×10^{-2}	6.78×10^{-4}	6.94×10^{-4}

Table 2
pH, ionic strength, and alkalinity for ferrihydrite samples

pH	Ionic strength (M)	Measured alkalinity (eq/L)	Calculated alkalinity (eq/L)
10^{-4} M Fe, 430 ppm CO_2, 10.9 mM $NaNO_3$, zero Ca			
7.40	1.11×10^{-2}	1.81×10^{-4}	1.80×10^{-4}
7.55	1.12×10^{-2}	2.64×10^{-4}	2.54×10^{-4}
7.85	1.14×10^{-2}	5.43×10^{-4}	5.19×10^{-4}
8.33	1.28×10^{-2}	1.71×10^{-3}	1.58×10^{-3}
8.44	1.31×10^{-2}	2.22×10^{-3}	2.04×10^{-3}
10^{-3} M Fe, 2.0% CO_2, 5 mM $NaNO_3$, zero Ca			
6.59	6.31×10^{-3}	1.17×10^{-3}	1.31×10^{-3}
6.82	7.22×10^{-3}	1.94×10^{-3}	2.22×10^{-3}
7.06	8.98×10^{-3}	3.44×10^{-3}	3.89×10^{-3}
7.34	1.36×10^{-2}	6.14×10^{-3}	7.50×10^{-3}
10^{-3} M Fe, 2.0% CO_2, 5 mM $NaNO_3$, 1.8 mM Ca			
6.11	1.08×10^{-2}	4.32×10^{-4}	4.27×10^{-4}
6.42	1.12×10^{-2}	8.95×10^{-4}	8.78×10^{-4}
6.63	1.18×10^{-2}	1.51×10^{-3}	1.43×10^{-3}
6.87	1.29×10^{-2}	2.30×10^{-3}	2.50×10^{-3}
7.08	1.45×10^{-2}	3.64×10^{-3}	4.08×10^{-3}

The Davies equation was used for activity correction of aqueous species only. Thermodynamic data used in the modeling are consistent with the most recent NEA database for uranium (Guillaumont et al., 2003), except the aqueous species, $CaUO_2(CO_3)_3^{2-}$ and $Ca_2UO_2(CO_3)_3^0$(aq) (Kalmykov and Choppin, 2000; Bernhard et al., 2001) were also included. Corrected to zero ionic strength, Bernhard et al. (2001) estimated values of 25.4 ± 0.3 and 30.6 ± 0.3 for the log of the formation constants for reactions (1)

and (2), respectively, and Kalmykov and Choppin (2000) estimated a value of 29.8 ± 0.7 for reaction (2):

$$Ca^{2+} + UO^{2+} + 3CO_3^{2-} = CaUO_2(CO_3)_3^{2-} \quad (1)$$

$$2Ca^{2+} + UO^{2+} + 3CO_3^{2-} = Ca_2UO_2(CO_3)_3^{0}(aq) \quad (2)$$

To be consistent with the new NEA database (Guillaumont et al., 2003), the log K values for reactions (1) and (2) were corrected upwards by 0.24 log unit (V. Brendler, personal communication). For reaction (2), the value of Kalmykov and Choppin (2000) was chosen for modeling calculations because it gave a better prediction of the experimental data for U(VI) sorption on quartz in the presence of Ca. The surface complexation modeling parameters used are presented in Table 3. Because the measured alkalinity generally agreed with the calculated alkalinity (Tables 1 and 2), the model calculations assumed that the aqueous phase was in equilibrium with respect to the known partial pressure of CO_2 in the gas phase.

The surface complexation model calculations presented here are *predictions* only of the effects of Ca (no data fitting), based on models calibrated in the absence of Ca (Table 3). The quartz and ferrihydrite solids used in the experiments in the absence of Ca (Waite et al., 1994; M. Kohler, unpublished results) were prepared using the same methods as in the experiments reported here.

3. Results and discussion

3.1. Aqueous speciation

Fig. 1 shows the equilibrium aqueous speciation as a function of pH for 1 μM U(VI) under the three experimental conditions that contain added Ca^{2+}. In each case, the $Ca_2UO_2(CO_3)_3^{0}(aq)$ species accounts for more than 50% of the U(VI) aqueous species in the alkaline pH range. The pH at which this species becomes predominant depends on the Ca^{2+} concentration, the partial pressure of carbon dioxide gas, and the ionic strength. The $CaUO_2(CO_3)_3^{2-}$ species is also present, but at much lower concentrations (Fig. 1).

3.2. Kinetics

The adsorption of U(VI) onto quartz in the presence of 8.9 mM Ca is quite rapid and reaches equilibrium within 8 h (Fig. 2a). The same is true in the absence of Ca (M. Kohler, unpublished results). Si is released into solution and dissolved Si seems to be almost linear with respect to time for the first 168-h before beginning to level off (Fig. 2b). In the case of ferrihydrite, U(VI) adsorption increased rapidly for the first 24 h, then continued slowly for up to 168 h (Fig. 2a), as was also observed by Waite et al. (1994). We chose a 48-h reaction time for both the

Table 3
Surface complexation model parameters

Model	Surface species	Exponents in mass law defining the surface species[A]						Log $K_f(I=0)$
		a	b	c	d	e	f	
Quartz TLM[B] 0.005–0.1 M $NaNO_3$, U(VI): 10^{-8}–10^{-5} M, pH: 3.5–9.0, pCO_2: air–7.5%	SO^-	1	−1			−1		−8.40
	SO^-Na^+	1	−1			−1	1	−6.51
	$SO_{strong}UO_2^+$	1	−1		1	1		1.98
	$SO_{weak}UO_2^+$	1	−1		1	1		−2.08
	$SO_{strong}UO_2OH$	1	−2		1			−1.88
	$SO_{weak}UO_2OH$	1	−2		1			−5.76
	$SO_{weak}UO_2(OH)(CO_3)^{2-}$	1	−4	1	1		−2	−14.2
Ferrihydrite TLM[C] 0.004–0.5 M $NaNO_3$U(VI): 10^{-8}–10^{-4} M, pH: 3.5–9.0, pCO_2: air–2%	SOH_2^+	1	1			1		5.10
	SO^-	1	−1			−1		−10.7
	$SOH_2^+NO_3^-$	1	1			1	−1	6.90
	SO^-Na^+	1	−1			−1	1	−9.00
	$SOCa$[D]	1	−1			0.4	0.6	−7.1
	$(SO^-)_2Ca^{2+}$[D]	2	−2			−2	2	−10.2
	$(SO_{strong})_2UO_2$	1	−2		1			−2.20
	$(SO_{weak})_2UO_2$	1	−2		1			−5.79
	$(SO_{strong})_2UO_2CO_3^{2-}$	1	−4	1	1	−0.6	−1.4	−12.3
	$(SO_{weak})_2UO_2CO_3^{2-}$	1	−4	1	1	−0.6	−1.4	−15.6

[A] Mass law for formation of the surface species is: [Surface species] = $K_f[SOH]^a(H^+)^b(H_2CO_3)^c(UO_2^{2+})^d\exp\{(-F/RT)(e\Psi_o+f\Psi_\beta)\}$. Coefficients for Na^+, Ca^{2+}, and NO_3^- not shown.

[B] TLM = triple layer model, $C_1 = 1.0$ F/m^2, $C_2 = 0.2$ F/m^2, total sites = 7.647 μmol/m^2; strong sites = 0.00306 μmol/m^2.

[C] TLM = triple layer model; $C_1 = 1.4$ F/m^2, $C_2 = 0.2$ F/m^2, surface area of ferrihydrite = 600 m^2/g $Fe_2O_3 \cdot H_2O$; total sites = 0.875 mol sites/mol Fe(III) as ferrihydrite; strong sites = 0.9625 sites/mmol Fe(III); U(VI) surface species form bidentate bonds that consume two surface sites in mass balance for sites but have an exponent of one in the mass law.

[D] Formation constants for Ca sorption calibrated with datasets of Figs. 2a and b in Cowan et al. (1991), to be consistent with the TLM parameters used in the ferrihydrite model. Best fit of the Ca sorption data was with one inner sphere and one outer sphere species, as also observed by Cowan et al. (1991).

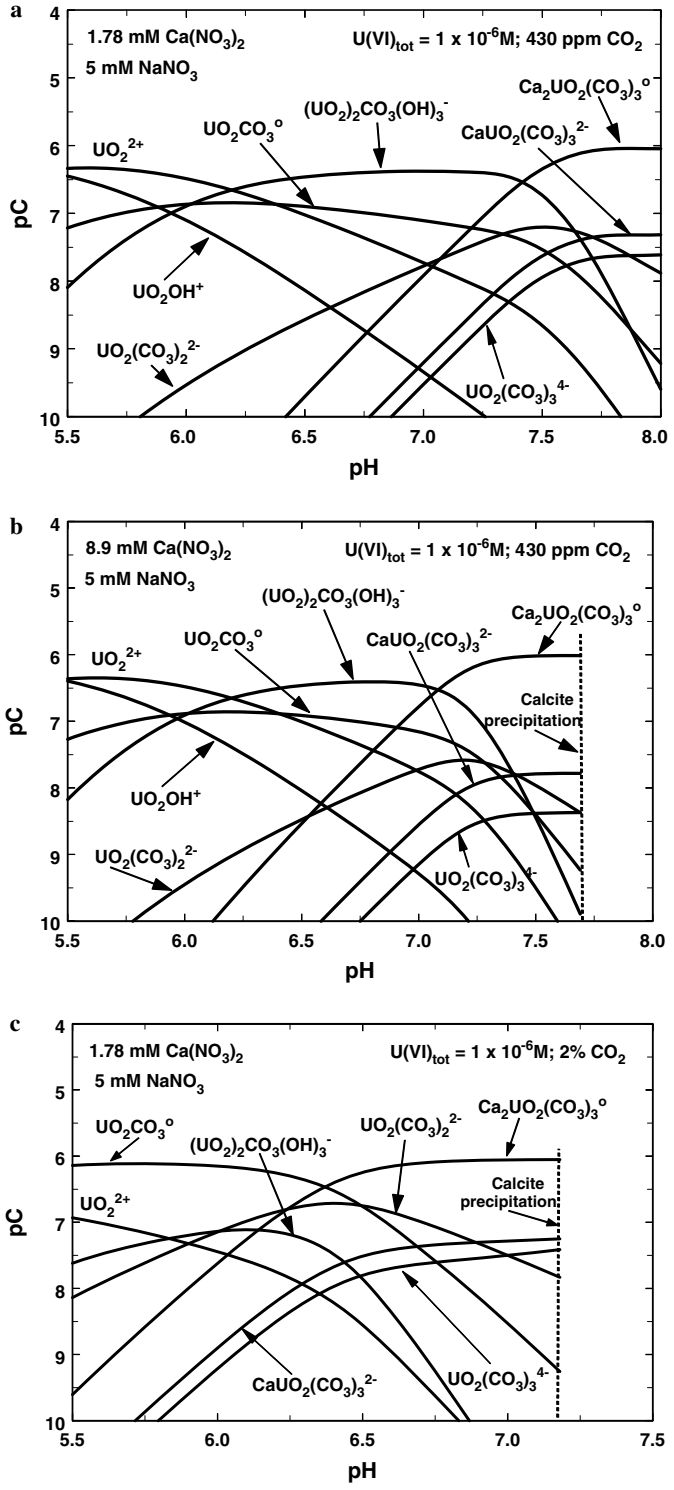

Fig. 1. Aqueous speciation of 1 μM U(VI), expressed as the log of species concentration (pC), as a function of pH in various solutions containing Ca^{2+} ion. A log K value of 30.0 for the $Ca_2UO_2(CO_3)_3^0$(aq) species (Eq. 2) was used for the calculations. (a) Aqueous phase equilibrated with the partial pressure of carbon dioxide in laboratory air (430 ppm) and containing 1.8 mM Ca. Solution is undersaturated with calcite for pH < 7.99. (b) Aqueous phase equilibrated with the partial pressure of carbon dioxide in air and containing 8.9 mM Ca. Solution is undersaturated with calcite for pH < 7.69. (c) Aqueous phase equilibrated with 2% CO_2(g) and containing 1.8 mM Ca. Solution is undersaturated with calcite for pH < 7.18.

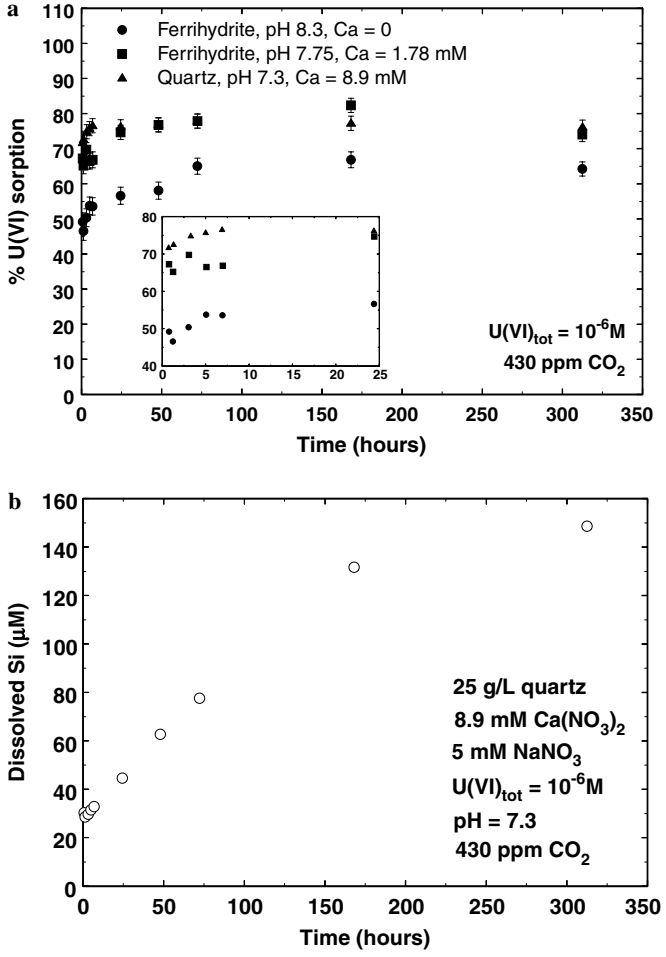

Fig. 2. Kinetics of 1 μM U(VI) adsorption onto ferrihydrite and quartz in the presence and absence of Ca^{2+} in 5 mM $NaNO_3$ solution in equilibrium with laboratory air (430 ppm CO_2). (a) U(VI) sorption as a function of time to ferrihydrite (10^{-4} M Fe) was studied in the absence of Ca at pH 8.30 (circles) and in the presence of 1.8 mM Ca at pH 7.75 (squares). U(VI) sorption onto quartz was studied in the presence of 8.9 mM Ca at pH 7.30 (triangles). (b) Dissolved Si is shown as a function of time in U(VI) sorption experiments with quartz in 8.9 mM $Ca(NO_3)_2$ solution at pH 7.3. Error bars are smaller than the symbols in this figure.

quartz and ferrihydrite systems, which corresponds to approximately 100% of the total adsorption for quartz and 98% for ferrihydrite in the presence of Ca. This reaction time was also chosen by Waite et al. (1994) and makes direct comparison with that data set straightforward.

3.3. Quartz

In the absence of Ca, U(VI) sorption to quartz decreased from about 90% at pH 7 to near zero at pH 8.75 (Fig. 3). Ionic strength (5 mM versus 32 mM) and the addition of dissolved silicate had negligible effects on U(VI) sorption. In the presence of 1.8 mM Ca, U(VI) sorption was significantly lower at pH > 7.0 than in the absence of Ca. A greater concentration of Ca (8.9 mM) lowered U(VI) sorption even more. For instance, at pH 7.7, U(VI) sorption decreased from 77% in the absence of Ca

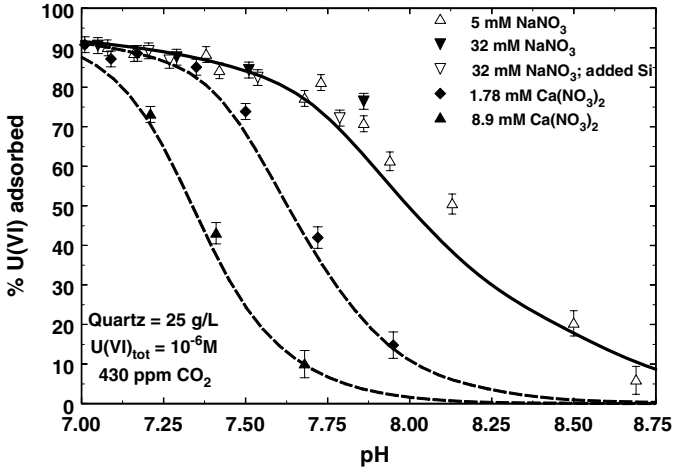

Fig. 3. U(VI) sorption on quartz (25 g/L) as a function of pH, ionic strength, and $Ca(NO_3)_2$ concentration in solutions with 1 μM total U(VI) and with the partial pressure of carbon dioxide in laboratory air (430 ppm CO_2). Open upward and filled downward triangles represent measurements of U(VI) sorption in 5 and 32 mM $NaNO_3$ solution, respectively, with no added Ca. Open downward triangles show data for U(VI) in 32 mM $NaNO_3$ solution with added silicate anion. Diamonds represent U(VI) sorption from a solution containing 5 mM $NaNO_3$ and 1.8 mM $Ca(NO_3)_2$, and filled upward triangles are for U(VI) sorption from a solution containing 5 mM $NaNO_3$ and 8.9 mM $Ca(NO_3)_2$. The solid line represents the predicted pH dependence of U(VI) sorption on 25 g/L quartz in 32 mM $NaNO_3$ solution equilibrated with 430 ppm CO_2 using a model calibrated in the absence of Ca (Table 3). Long-dashed curves represent the predicted pH dependence of U(VI) sorption with 1.8 and 8.9 mM added Ca, with log K of the formation constant for the aqueous $Ca_2UO_2(CO_3)_3^0$ species equal to 30.0.

to 42% and 10% in the presence of 1.8 and 8.9 mM Ca, respectively. As shown in Figs. 1a and b, thermodynamic calculations suggest that the addition of Ca changes the aqueous speciation of U(VI), with the $Ca_2UO_2(CO_3)_3^0$(aq) species becoming predominant at pH values of about 7.2 (8.9 mM Ca) and 7.4 (1.78 mM Ca). It can be seen in Fig. 3 that the first decrease in U(VI) sorption (relative to the system with Ca = 0) is observed near these pH values for the respective Ca concentrations.

The quartz surface complexation model (Table 3) used here is based on U(VI) sorption experiments conducted in the absence of Ca^{2+}. The model prediction of U(VI) sorption on 25 g/L quartz in the absence of Ca (Fig. 3, solid line) is in good agreement with the data in the pH range 7–8.75. The long dash curves in Fig. 3 show the model predictions of U(VI) sorption using the formation constant of 30.0, corrected from Kalmykov and Choppin (2000) for Eq. (2). The calculations at 1.8 and 8.9 mM Ca predict the observed decrease in U(VI) sorption very well. The calculations are quite sensitive to the value of the formation constant for the $Ca_2UO_2(CO_3)_3^0$(aq) aqueous species; using the log value of 30.8 for the constant (Bernhard et al., 2001) results in a much larger decrease in U(VI) sorption than was observed. However, given the uncertainty in the value of the formation constant for the $Ca_2UO_2(CO_3)_3^0$(aq) species, the effect of Ca on U(VI) sorption by quartz is well predicted by considering only the changes caused in U(VI) aqueous speciation (and thus, assuming that $Ca_xUO_2(CO_3)_3$ aqueous species are not sorbed by the quartz surface). This is a reasonable assumption, since the $Ca_2UO_2(CO_3)_3^0$(aq) aqueous species is uncharged and unlikely to bond with the surface via the Ca atoms, because they are already bonded to oxygen atoms of the carbonate anions (Bernhard et al., 2001). The $CaUO_2(CO_3)_3^{2-}$ species is also unlikely to adsorb for the same reason and is present at much lower concentrations (Fig. 1).

Ca sorption in the pH range 6–8 was negligible on the quartz, and thus, the decrease in U(VI) sorption observed in the presence of Ca is not due to surface site competition. Si was dissolved/released during the sorption experiments, and in experiments with Ca, greater concentrations of Si were measured in solution (Fig. 4). It is well documented that the presence of alkali and alkaline earth cations increase dissolution rates of quartz, and in some cases, increases the solubility (Barker et al., 1994; Dove and Rimstidt, 1994; House, 1994; Dove and Nix, 1997). However, as shown in Fig. 3, the addition of dissolved silicate had no observable effect on U(VI) sorption in the pH range studied. Since site competition with Ca^{2+}, ionic strength, and dissolved silicate can be discounted as factors, the observed decrease in U(VI) sorption in the presence of Ca must be due to the predicted changes in U(VI) aqueous speciation.

3.4. Ferrihydrite

Sorption of 1 μM U(VI) on ferrihydrite was measured as a function of pH and Ca concentration under two sets of chemical conditions: (a) with 10^{-4} M Fe as ferrihydrite in systems equilibrated with air (430 ppm CO_2) and (b) with 10^{-3} M Fe as ferrihydrite in systems equilibrated with 2% CO_2 gas.

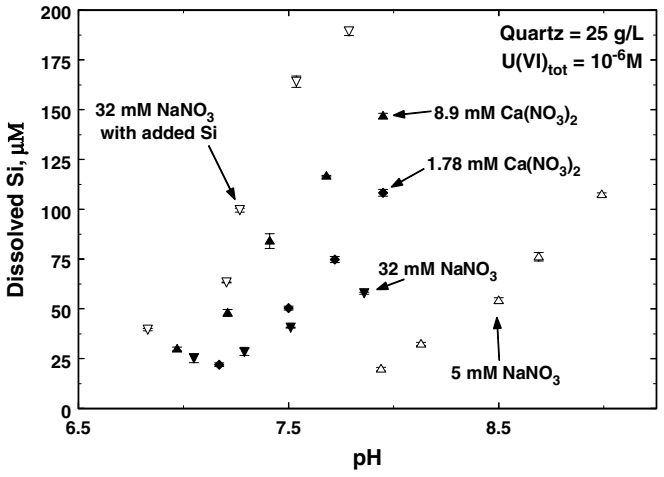

Fig. 4. Concentration of dissolved Si after 72 h of batch equilibration during U(VI) sorption experiments as a function of pH and added Ca concentration. Systems equilibrated with air. Symbols are consistent with those in Fig. 3.

Sorption of U(VI) onto ferrihydrite (at 10^{-4} M Fe) was lower in the presence of 1.8 mM Ca in the pH range 7.3–8.0 in comparison to a 10.9 mM $NaNO_3$ solution (no Ca) of similar ionic strength (Fig. 5). Experiments were not conducted above pH 8 in the presence of Ca because calcite precipitation is predicted at pH > 7.99 for these conditions. Like the results observed for quartz, the decrease in U(VI) sorption becomes apparent near the pH value at which the $Ca_2UO_2(CO_3)_3^0$(aq) species becomes predominant (Fig. 1a). Ca^{2+} sorption was not detectable in any of the experiments with ferrihydrite, but it is known that Ca^{2+} sorbs to the ferrihydrite surface under certain conditions (Kinniburgh et al., 1975; Dempsey and Singer, 1980; Cowan et al., 1991) and would be expected to influence surface charge (Davis and Kent, 1990).

Surface complexation model predictions are shown for the effect of Ca on U(VI) sorption in Fig. 5, including formation of the aqueous $Ca_xUO_2(CO_3)_3$ species, both with and without consideration of Ca^{2+} sorption. A Ca^{2+} sorption model for ferrihydrite was derived for these calculations based on a fit to experimental data in Cowan et al. (1991), using parameters consistent with the U(VI) sorption model for ferrihydrite (Table 3). The model calculations over-predict the effect of Ca caused by formation of the Ca_2UO_2 $(CO_3)_3^0$(aq) species, unless Ca^{2+} sorption is also considered. Including Ca^{2+} sorption in the model calculations affects the predicted surface charge of the ferrihydrite, causing the electrical potential to increase in the β plane in comparison to the calculations without Ca^{2+} sorption. Because one of the U(VI) surface species has a negative charge (i.e., $(SO)_2UO_2CO_3^{2-}$), the increase in electrical potential in the β plane has a favorable influence on formation of the ternary-uranyl-carbonato surface complex. Thus, inclusion of Ca^{2+} sorption in the model calculations improves the prediction of the net effect of Ca on U(VI) sorption.

A second set of conditions (10^{-3} M Fe as ferrihydrite; 2% CO_2) was also tested for the effect of Ca on U(VI) sorption (Fig. 6). Equilibration with the higher partial pressure of CO_2(g) shifts the sorption edge for U(VI) in the absence of Ca to a lower pH range (compare Figs. 5 and 6), as was observed by Waite et al. (1994). The presence of 1.8 mM Ca decreased U(VI) sorption in the pH range 6.7–7.2 under these conditions in comparison to a 5 mM $NaNO_3$ solution (Fig. 6). Experiments were not conducted above pH 7.2 in the presence of 1.8 mM Ca and 2% CO_2 because of calcite precipitation. For these conditions, the effect of Ca is not apparent at the pH value (6.3) at which the $Ca_2UO_2(CO_3)_3^0$(aq) species becomes predominant (Fig. 1c), but this might be obscured by the fact that the decrease is negligible when U(VI) sorption is very strong (near 100% adsorbed). The surface complexation model predictions of the effect of Ca were in reasonable agreement with the experimental observations (Fig. 6). As before, the predicted effect of Ca addition to the system is caused by two processes: (a) the formation of $Ca_2UO_2(CO_3)_3^0$(aq) species, which decreases U(VI) adsorption and (b) Ca^{2+} sorption, which increases U(VI) adsorption by increasing the electrical potential in the β plane. The net result under these conditions is a decrease in U(VI) sorption.

In general, the largest effect of Ca on U(VI) sorption was observed when U(VI) sorption was less than 100% and the pH was at a value at which the $Ca_2UO_2(CO_3)_3^0$(aq) species

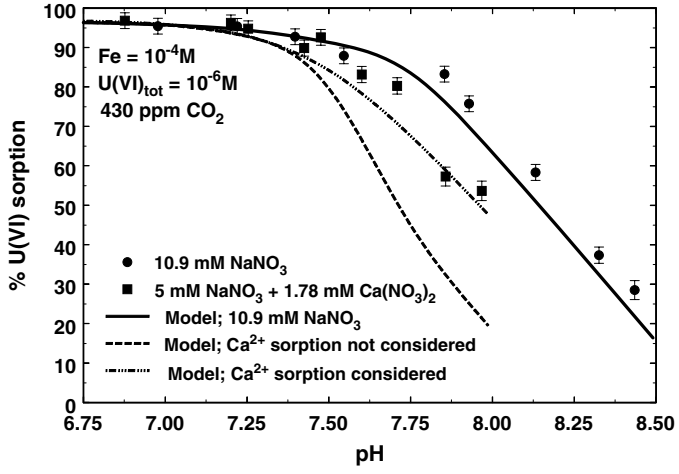

Fig. 5. U(VI) sorption by ferrihydrite (10^{-4} M Fe) in equilibrium with air as a function of pH in 5 mM $NaNO_3$ and 1.8 mM $Ca(NO_3)_2$ (squares) and 10.9 mM $NaNO_3$ (circles). The solid line represents the predicted pH dependence of U(VI) sorption in the absence of Ca using the model given in Table 3. Long-dashed curve represents the predicted pH dependence of U(VI) sorption with 1.8 mM added Ca, with the log K of the formation constant for the aqueous $Ca_2UO_2(CO_3)_3^0$ species equal to 30.0 and without Ca^{2+} sorption considered. The dot-dot-dash curve represents the same conditions with Ca^{2+} sorption considered.

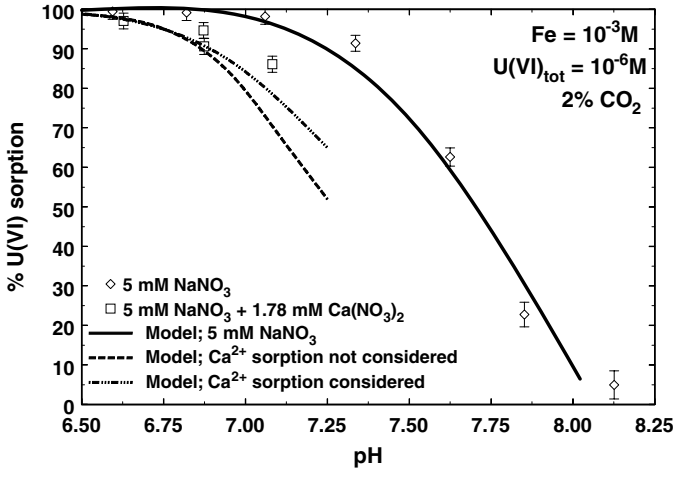

Fig. 6. U(VI) sorption by ferrihydrite (10^{-3} M Fe) in 5 mM $NaNO_3$ solution equilibrated with 2% CO_2 as a function of pH in the presence (open squares) and absence (open diamonds) of 1.8 mM $Ca(NO_3)_2$. Solid line represents the predicted pH dependence of U(VI) sorption in the absence of Ca using the model given in Table 3. Long-dashed curve represents the predicted pH dependence of U(VI) sorption with 1.8 mM added $Ca(NO_3)_2$, with log K of the formation constant for the aqueous $Ca_2UO_2(CO_3)_3^0$ species equal to 30.0 and without Ca^{2+} sorption considered. The dot-dot-dash curve represents the same conditions with Ca^{2+} sorption considered.

was predicted to dominate U(VI) aqueous speciation. The predominance of the $Ca_2UO_2(CO_3)_3^0$(aq) species is sensitive to factors such as pH, Ca concentration, and the partial pressure of carbon dioxide gas, but is also very sensitive to ionic strength because of the high charge of the $UO_2(CO_3)_2^{2-}$ and $UO_2(CO_3)_3^{4-}$ species (Fig. 1). The effect of Ca on U(VI) adsorption on quartz is greater than the effect on ferrihydrite under the conditions studied. This is most likely due to the high surface area and strong U(VI) adsorption by ferrihydrite. The experimental data and model predictions of the effect of Ca on U(VI) sorption were in good agreement when the formation constants of the aqueous species $CaUO_2(CO_3)_3^{2-}$ and $Ca_2UO_2(CO_3)_3^0$(aq) were included in the surface complexation modeling predictions. It is unlikely that either the $CaUO_2(CO_3)_3^{2-}$ or $Ca_2UO_2(CO_3)_3^0$(aq) aqueous species adsorb via the Ca atoms to the ferrihydrite surface because the Ca atoms are already bonded to oxygen atoms of the carbonate anions (Bernhard et al., 2001).

The results demonstrate that the presence of Ca^{2+} in solution can decrease U(VI) sorption on ferrihydrite and quartz under conditions at which the $Ca_2UO_2(CO_3)_3^0$(aq) species dominates U(VI) aqueous speciation. Such conditions are prevalent in many uranium-contaminated aquifers (Bernhard et al., 2001; Brooks et al., 2003; Davis and Curtis, 2003; Davis et al., 2004; Wang et al., 2004). The data and modeling calculations illustrate that it is important to take into account the effect of Ca on U(VI) aqueous speciation when predicting the sorption and mobility of U(VI) at contaminated sites.

Acknowledgments

This research was supported by the US Department of Energy (DOE)–Environmental Management (EM) through the Hanford Remediation and Closure Science Project and the Office of Biological and Environmental Research (OBER) through the EMSP program. The authors thank Chris Fuller, Harvey Doner and anonymous reviewers for helpful reviews of draft versions of this manuscript. We also thank Matthias Kohler for providing assistance with the quartz experiments and modeling. The use of trade names in this paper is for identification purposes only and does not constitute endorsement by the US Geological Survey.

Associate editor: George R. Heltz

References

Barker, P., Fontes, J.C., Gasse, F., Druart, J.C., 1994. Experimental dissolution of diatom silica in concentrated salt solutions and implications for paleoenvironmental reconstruction. *Limnol. Oceanogr.* **39**, 99–110.

Barnett, M.O., Jardine, P.M., Brooks, S.C., 2002. U(VI) adsorption to heterogeneous subsurface media: application of a surface complexation model. *Environ. Sci. Technol.* **36**, 937–942.

Barnett, M.O., Jardine, P.M., Brooks, S.C., Selim, H.M., 2000. Adsorption and transport of uranium(VI) in subsurface media. *Soil Sci. Soc. Am. J.* **64**, 908–917.

Bernhard, G., Geipel, G., Brendler, V., Nitsche, H., 1996. Speciation of uranium in seepage waters of a mine tailing pile studied by time-resolved laser-induced fluorescence spectroscopy (TRLFS). *Radiochim. Acta* **74**, 87–91.

Bernhard, G., Geipel, G., Reich, T., Brendler, V., Amayri, S., Nitsche, H., 2001. Uranyl(VI) carbonate complex formation: validation of the $Ca_2UO_2(CO_3)_3$(aq.) species. *Radiochim. Acta* **89**, 511–518.

Brooks, S.C., Fredrickson, J.K., Carroll, S.L., Kennedy, D.W., Zachara, J.M., Plymale, A.E., Kelly, S.D., Kemner, K.M., Fendorf, S., 2003. Inhibition of bacterial U(VI) reduction by calcium. *Environ. Sci. Technol.* **37**, 1850–1858.

Cowan, C.E., Zachara, J.M., Resch, C.T., 1991. Cadmium adsorption on iron oxides in the presence of alkaline-earth elements. *Environ. Sci. Technol.* **25**, 437–446.

Crowley, K.D., Ahearne, J.F., 2002. Managing the environmental legacy of U.S. nuclear weapons production. *Am. Sci.* **90**, 514–523.

Curtis, G.P., Fox, P., Kohler, M., Davis, J.A., 2004. Comparison of in situ uranium K_D values with a laboratory determined surface complexation model. *Appl. Geochem.* **19**, 1643–1653.

Davis, J.A., Curtis, G.P., 2003. Application of surface complexation modeling to describe uranium(VI) adsorption and retardation at the uranium mill tailings site at Naturital, Colorado. US Nuclear Regulatory Commission. NUREG/CR-6708.

Davis, J.A., Kent, D.B., 1990. Surface complexation modeling in aqueous geochemistry: mineral-water interface geochemistry. *Rev. Mineral* **23**, 177–260.

Davis, J.A., Meece, D.E., Kohler, M., Curtis, G.P., 2004. Approaches to surface complexation modeling of uranium(VI) adsorption on aquifer sediments. *Geochim. Cosmochim. Acta* **68**, 3621–3641.

Dempsey, B.A., Singer, P.C., 1980. The effects of calcium on the adsorption of zinc by MnO_x(s) and $Fe(OH)_3$(am). In: Baker, R.A. (Ed.), *Contaminants and Sediments*, vol. 2. Ann Arbor Science, pp. 333–352.

Dove, P.M., Nix, C.J., 1997. The influence of the alkaline earth cations, magnesium, calcium, and barium on the dissolution kinetics of quartz. *Geochim. Cosmochim. Acta* **61**, 3329–3340.

Dove, P.M., Rimstidt, J.D., 1994. Silica–water interactions. In: Heaney, P.J., Prewitt, C.T., Gibbs, G.V. (Eds.), *Silica: Physical Behavior, Geochemistry and Materials Applications*. Mineralogical Society of America, pp. 259–308.

Duff, M.C., Amrhein, C., 1996. Uranium(VI) adsorption on goethite and soil in carbonate solutions. *Soil Sci. Soc. Am. J.* **60**, 1393–1400.

Guillaumont, R., Fanghanel, T., Neck, V., Fuger, J., Palmer, D.A., Grenthe, I., Rand, M.H., 2003. *Update on the Chemical Thermodynamics of Uranium, Neptunium, Plutonium, Americium, and Technetium*. Elsevier, Amsterdam.

Herbelin, A.L., Westall, J.C., 1999. *FITEQL: A Computer Program for the Determination of Chemical Equillibrium Constants from Experimental Data*. Chemistry Department, Oregon State University, Corvallis, OR.

House, W.A., 1994. The role of surface complexation in the dissolution kinetics of silica: effects of monovalent and divalent ions at 25 °C. *J. Colloid Interface Sci.* **163**, 379–390.

Hsi, C.D., Langmuir, D., 1985. Adsorption of uranyl onto ferric oxyhydroxides: application of the surface complexation site-binding model. *Geochim. Cosmochim. Acta* **49**, 1931–1941.

Kalmykov, N., Choppin, G.R., 2000. Mixed $Ca^{2+}/UO_2^{2+}/CO_3^{2-}$ complex formation at different ionic strengths. *Radiochim. Acta* **88**, 603–606.

Kinniburgh, D.G., Syers, J.K., Jackson, M.L., 1975. Specific adsorption of trace amounts of calcium and strontium by hydrous oxides of iron and aluminum. *Soil Sci. Soc. Am. Proc.* **39**, 464–470.

Kohler, M., Curtis, G.P., Kent, D.B., Davis, J.A., 1996. Experimental investigation and modeling of uranium(VI) transport under variable chemical conditions. *Water Resour. Res.* **32**, 3539.

Kohler, M., Curtis, G.P., Meece, D.E., Davis, J.A., 2004. Methods for estimating adsorbed uranium(VI) and distribution coefficients in contaminated sediments. *Environ. Sci. Technol.* **38**, 240–247.

Pabalan, R.T., Turner, D.R., Bertetti, F.P., Prikryl, J.D., 1998. Uranium^{VI} sorption onto selected mineral surfaces: key geochemical parameters. In: Jenne, E.A. (Ed.), *Adsorption of Metals by Geomedia: Variables, Mechanisms, and Model Applications*. Academic Press, San Diego, CA, USA, pp. 99–130.

Payne, T.E., 1999. Uranium(VI) interactions with mineral surfaces: controlling factors and surface complexation modeling. Ph.D. thesis, University of New South Wales, Australia.

Riley, R.G., Zachara, J.M., Wobber, F.J., 1992. Chemical contaminants on DOE lands and selection of contaminant mixtures for subsurface science research. U.S. Department of Energy, DOE/ER-0547T.

Turner, G.D., Zachara, J.M., McKinley, J.P., Smith, S.C., 1996. Surface-charge properties and UO_2^{2+} adsorption of a subsurface smectite. *Geochim. Cosmochim. Acta* **60**, 3399–3414.

Waite, T.D., Davis, J.A., Payne, T.E., Waychunas, G.A., Xu, N., 1994. Uranium(VI) adsorption to ferrihydrite: application of a surface complexation model. *Geochim. Cosmochim. Acta* **58**, 5465–5478.

Wang, Z., Zachara, J.M., Yantasee, W., Gassman, P.L., Liu, C., Joly, A.G., 2004. Cryogenic laser induced fluorescence characterization of U(VI) in Hanford vadose zone pore waters. *Environ. Sci. Technol.* **38**, 5591–5597.

Zheng, Z., Tokunaga, T.K., Wan, J., 2003. Influence of calcium carbonate on U(VI) sorption to soils. *Environ. Sci. Technol.* **37**, 5603–5608.